

A distributed feedback silicon evanescent laser

Alexander W. Fang, Erica Lively, Ying-Hao Kuo, Di Liang, John. E. Bowers

¹University of California, Santa Barbara, Department of Electrical and Computer Engineering, Santa Barbara, CA 93106, USA
awfang@ece.ucsb.edu

Abstract: We report an electrically pumped distributed feedback silicon evanescent laser. The laser operates continuous wave with a single mode output at 1600 nm. The laser threshold is 25 mA with a maximum output power of 5.4 mW at 10 °C. The maximum operating temperature and minimum line width of the laser are 50 °C, and 3.6 MHz, respectively.

©2008 Optical Society of America

OCIS codes: (140.5960) Semiconductor lasers; (250.5300) Photonic integrated circuits.

References and links

1. A. W. Fang, H. Park, O. Cohen, R. Jones, M. J. Paniccia, and J. E. Bowers, "Electrically pumped hybrid AlGaInAs-silicon evanescent laser," *Opt. Express* **14**, 9203-9210 (2006).
2. J. Van Campenhout, P. Rojo Romeo, P. Regreny, C. Seassal, D. Van Thourhout, S. Verstyuyft, L. Di Cioccio, J. -M. Fedeli, C. Lagahe, and R. Baets, "Electrically pumped InP-based microdisk lasers integrated with a nanophotonic silicon-on-insulator waveguide circuit," *Opt. Express* **15**, 6744-6749 (2007).
3. T. Maruyama, T. Okumura, S. Sakamoto, K. Miura, Y. Nishimoto, and S. Arai, "GaInAsP/InP membrane BH-DFB lasers directly bonded on SOI substrate," *Opt. Express* **14**, 8184-8188 (2006) <http://www.opticsinfobase.org/abstract.cfm?URI=oe-14-18-8184>.
4. G. Morthier, P. Vankwikelberge, *Handbook of Distributed Feedback Laser Diodes* (Arctech House, Norwood, MA, 1997).
5. A. Liu, L. Liao, D. Rubin, J. Basak, H. Nguyen, Y. Chetrit, R. Cohen, N. Izhaky, and M. Paniccia, "High-Speed Silicon Modulator for Future VLSI Interconnect," in *Integrated Photonics and Nanophotonics Research and Applications*, OSA Technical Digest (CD) (Optical Society of America, 2007), paper IMD3.
6. H. Park, Y.-H. Kuo, A. W. Fang, R. Jones, O. Cohen, M. J. Paniccia, J. E. Bowers, "A hybrid AlGaInAs-silicon evanescent preamplifier and photodetector," *Opt. Express* **15**, No. 21, (2007).
7. H. Park, A. W. Fang, R. Jones, O. Cohen, M. J. Paniccia, and J. E. Bowers, "40 C Continuous-Wave Electrically Pumped Hybrid Silicon Evanescent Laser," International Semiconductor Laser Conference 2006 (ISLC 2006), post deadline paper, (2006)
8. H. Park, A. W. Fang, R. Jones, O. Cohen, O. Raday, M. N. Sysak, M. J. Paniccia, and J. E. Bowers, "A hybrid AlGaInAs-silicon evanescent waveguide photodetector," *Opt. Express* **15**, 6044-6052 (2007).
9. A. W. Fang, R. Jones, H. Park, O. Cohen, O. Raday, M. J. Paniccia, and J. E. Bowers, "Integrated AlGaInAs-silicon evanescent race track laser and photodetector," *Opt. Express* **15**, 2315-2322 (2007).
10. M. N. Sysak, H. Park, A. W. Fang, J. E. Bowers, R. Jones, O. Cohen, O. Raday, and M. J. Paniccia, "Experimental and theoretical thermal analysis of a Hybrid Silicon Evanescent Laser," *Opt. Express* **15**, 15041-15046 (2007).
11. D. Derrickson, *Fiber optic test and measurement* (Prentice Hall, 1998), page 185.

1. Introduction

Recently, new hybrid integration architectures have been developed, allowing for alignment free transfer of III-V materials to silicon, in order to fulfill the need of electrically pumped lasers for use in silicon photonic integrated circuits [1-3]. Distributed feedback lasers are attractive for these applications since they have a single longitudinal mode output and their short cavity lengths allow for low threshold currents while still producing output powers in the mW regime [4]. Figure 1 shows a concept for a silicon terabit transmitter utilizing hybrid integration. 25 distributed feedback lasers are externally modulated at 40 Gb/s [5] and then multiplexed together into a single waveguide to form a wavelength division multiplexed 1 Tb/s data stream. Although micro-disk lasers yield single wavelength output, their wavelength selection is determined by the round trip cavity length; a parameter strongly dependent on fabrication variations, making wavelength targeting a challenge. In addition, their small size

leads to high thermal impedance limiting the current maximum demonstrated continuous wave operating temperature on silicon to 20 °C [2]. Grating based lasers, on the other hand, are more dependent on grating periodicity rather than duty cycle for wavelength selection, giving them an increased wavelength targeting precision. Optically pumped III-V distributed feedback (DFB) membrane lasers on silicon-on-insulator (SOI) have been demonstrated with maximum output powers of 125 nW [3]. We report here the first electrically pumped DFB silicon evanescent laser (DFB-SEL). The laser operates CW up to 50 °C. Single wavelength lasing is observed at 1600 nm with a minimum linewidth of 3.6 MHz and maximum output power of 5.4 mW at 10 °C.

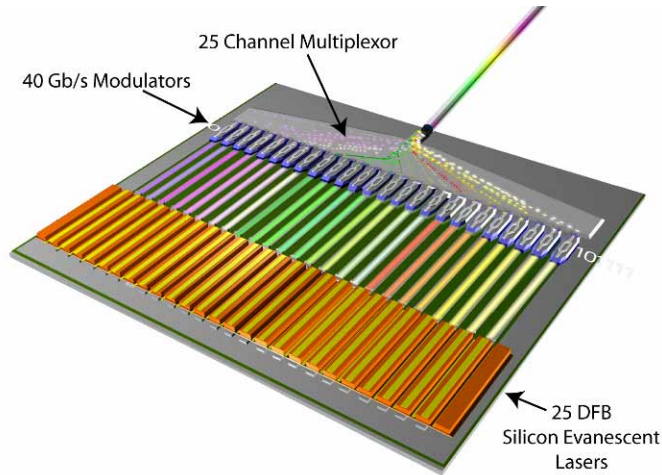


Fig. 1. A silicon terabit transmitter with 25 DFB-SELs externally modulated at 40 Gb/s.

2. Device design

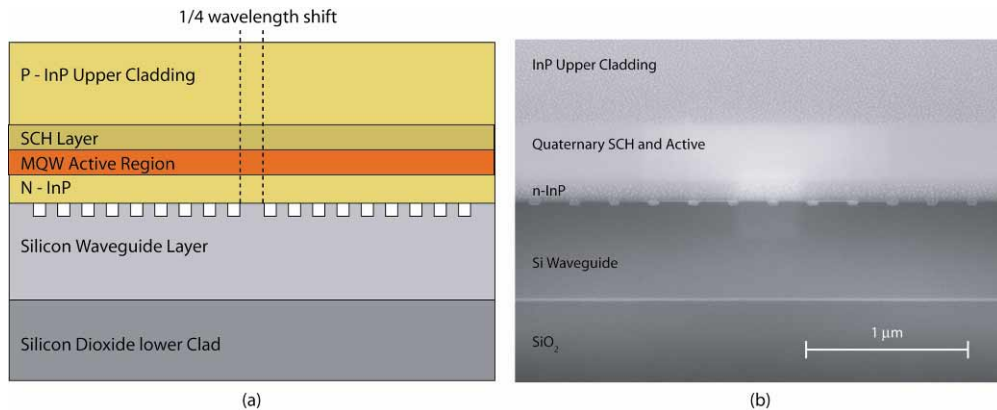


Fig. 2. (a) DFB-SEL longitudinal cross section diagram (b) Scanning electron microscope image of DFB-SEL longitudinal cross section.

The device is fabricated on the silicon evanescent device platform [6] with an AlGaInAs quantum well based active layer structure wafer bonded to silicon waveguides. Gratings are formed by depositing a 50 nm PECVD SiO₂ hard mask onto the un-patterned silicon on insulator wafer. The hard mask is patterned with electron-beam lithography and inductively coupled plasma dry etching to form a ~25 nm surface corrugated grating with a 238 nm pitch and 71 % duty cycle. The grating stop-band is designed at around 1600 nm, in order to account for the spectral peak shift to the 1600 nm range seen in previous devices due to device

heating [7]. Next, silicon waveguides are formed by depositing a 200 nm SiO₂ hard mask and patterning with projection lithography and a second ICP dry etch. The silicon waveguide has a width, height, and rib etch depth of 1.5 μm, 0.7 μm, and 0.5 μm, respectively. This yields a quantum well confinement factor of 5.2% and a silicon confinement factor of 59.2%. Next, the III-V structure is transferred to the silicon wafer with a low temperature wafer bonding technique and processed for electrical current flow control, the definition of passive regions through the selective removal of III-V materials, and the formation of tapers as described by H. Park et al. [6] Figure 2 shows a longitudinal cross section diagram of the laser structure and a cross sectional scanning electron microscope image of the fabricated device. The effective indices of the unetched region and the etched region are calculated using the film mode matching (FMM) method to be 3.3688 and 3.3441, respectively. This results in a grating κ of $\sim 247 \text{ cm}^{-1}$. The κ of these gratings are large when compared to the 73 cm^{-1} κ of surface corrugated gratings on passive silicon rib waveguides of similar dimensions since the index difference between air and silicon is quite large and the index perturbation is located near the center of the optical mode. The grating is 340 microns long with a $\frac{1}{4}$ wavelength shift in the center of the grating in order to break the modal degeneracy inside the distributed feedback Bragg gratings. The top of Fig. 3 shows the device layout. The DFB-SEL consists of a 14 μm wide and 200 μm long gain region. N contacts are placed above and below the III-V mesa while p contacts are placed on top of the mesa. The probe pads are not drawn on this diagram for simplicity but are shown in the microscope image. 80 μm long tapers are formed by linearly narrowing the III-V mesa region above the silicon waveguide. This adiabatically transforms the mode from the hybrid waveguide to the passive silicon waveguide allowing for losses on the order of 1.2 dB per taper and reflections on the order of 6×10^{-4} [6]. Two tapers are placed on both ends of this gain region and are also electrically pumped, giving way for a small amount of optical gain. Silicon evanescent photo-detectors are placed on both sides of the laser in order to enable on chip testing of the DFB-SEL performance. The photo-detectors are 240 μm long including the two 80 μm long tapers. The detector to the right is placed 400 microns away in order to allow room for dicing and polishing for off chip spectral tests.

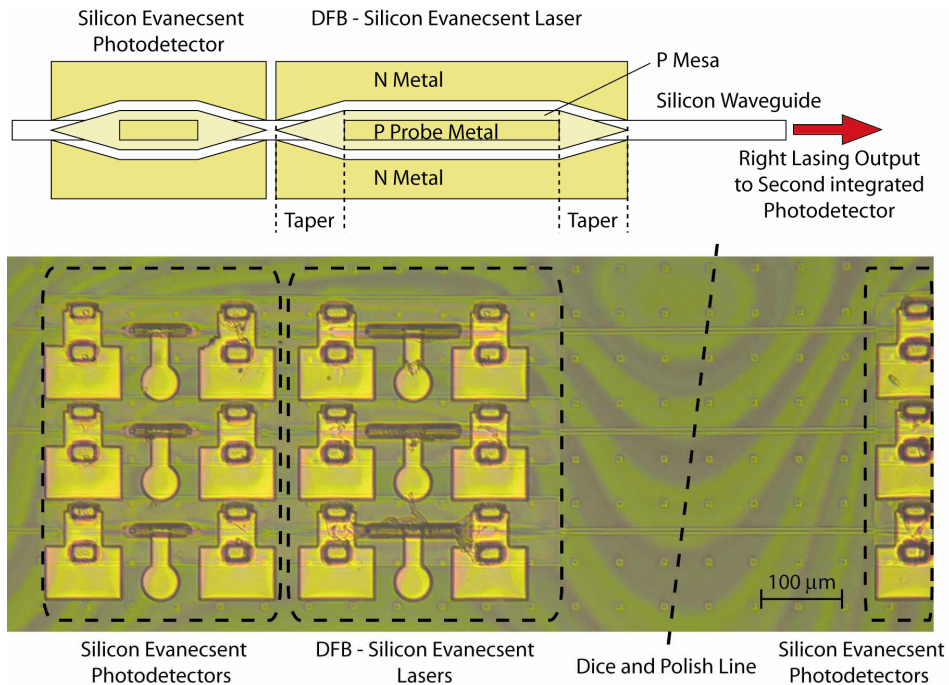


Fig. 3. (top) DFB-SEL device layout. (bottom) Microscope image of DFB-SEL and integrated silicon evanescent photo-detectors.

3. Experimental results

The light-current (L-I) characteristics of the DFB-SEL is measured on chip by collecting light out of both sides of the laser with integrated silicon evanescent photo-detectors. To determine the laser power output, we assume 100% internal quantum efficiency of the photodetectors [8] in order to conservatively assess the laser performance. It can be seen from Fig. 3 that at 10 °C, the lasing threshold is 25 mA, with a maximum output power of 5.4 mW. This corresponds to a threshold current density of 1.4 KA/cm², which is slightly lower than the 2 KA/cm² and 1.7 KA/cm² seen in previously demonstrated Fabry-Perot [1] and Racetrack [9] SELs, respectively. The maximum lasing temperature is 50 °C. We attribute the ripples in the L-I curve to instabilities caused by reflections off the right on-chip detector and observed that they disappear once the detector is diced off. The device heats as current injection levels are increased, changing the phase of the light reflected off the right detector. The secondary y-axis of Fig. 4 shows voltage-current curve with a laser turn on is ~1.8V. The laser has a 13 ohm device series resistance. This value scales appropriately with the 4.5 ohm resistance measured on 800 μm long Fabry-Perot lasers with similar III-V mesa dimensions. The lasing spectrum is taken by dicing off the right photo-detector, polishing, and anti-reflection coating the silicon waveguide output facet. Light is from the collected with a lensed fiber into an HP spectrum analyzer with a 0.08 nm resolution bandwidth. Figure 5 shows the spectrum with a 10 nm span with the laser being driven at 90 mA. The laser has a lasing peak of 1599.3 nm and a side-mode suppression ratio of 50 dB. It can be seen from the inset that the laser operates single mode over a 100 nm span.

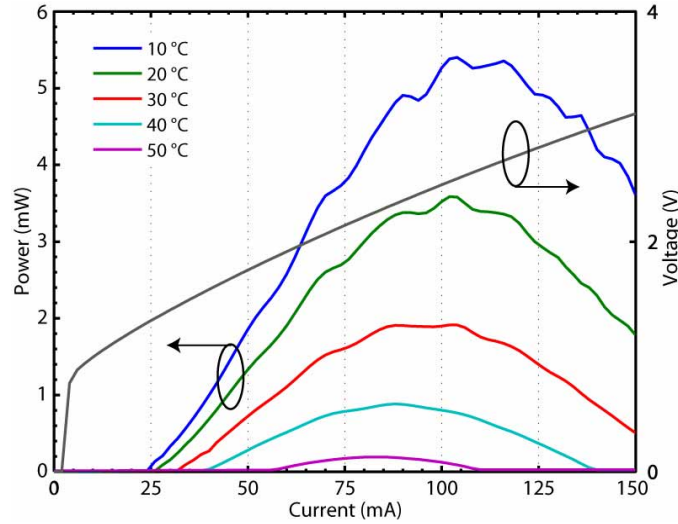


Fig. 4. – L-I-V curve for stage temperatures of 10 °C to 50 °C.

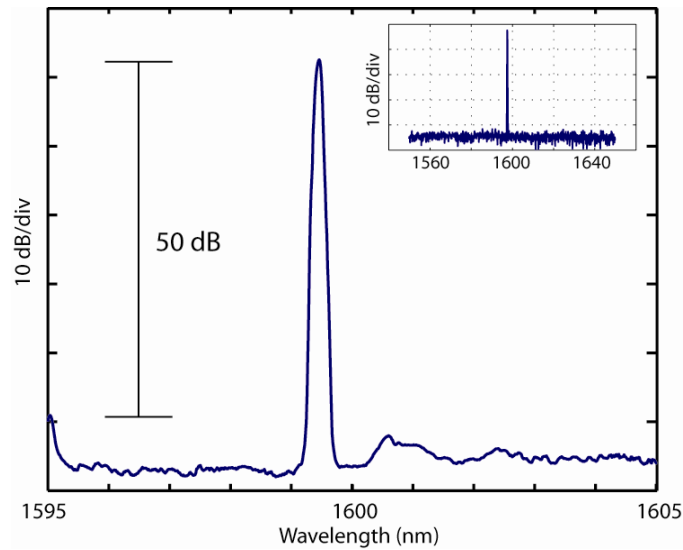


Fig. 5. The lasing spectrum at 90 mA injection current with a 50 dB side mode extinction ratio. (inset) The lasing spectrum over a 100 nm span showing single mode lasing.

The thermal impedance, Z_T , of the laser was determined by measuring the lasing peak shift as a function of electrical dissipated power (injection current \times device voltage) under continuous operation, and as a function of stage temperature under pulsed operation as described in ref [10]. Figure 6(a) shows the spectral shift under CW operation for various current levels. It can be seen that the laser stays single mode throughout the various current injection levels. Figure 6(b) shows the corresponding plot of wavelength versus electrical dissipated power with a 12.849 nm/W slope ($d\lambda/dP$). Figure 6(c) shows the change in lasing wavelength under pulsed operation as a function a stage temperature. $d\lambda/dT$ is measured at 0.0971 nm/°C. The resulting thermal impedance is 132 °C/W. This value is higher than the 40 °C/W measured on 850 micron long Fabry-Perot SELs but scales appropriately due to the DFB-SEL's short device length.

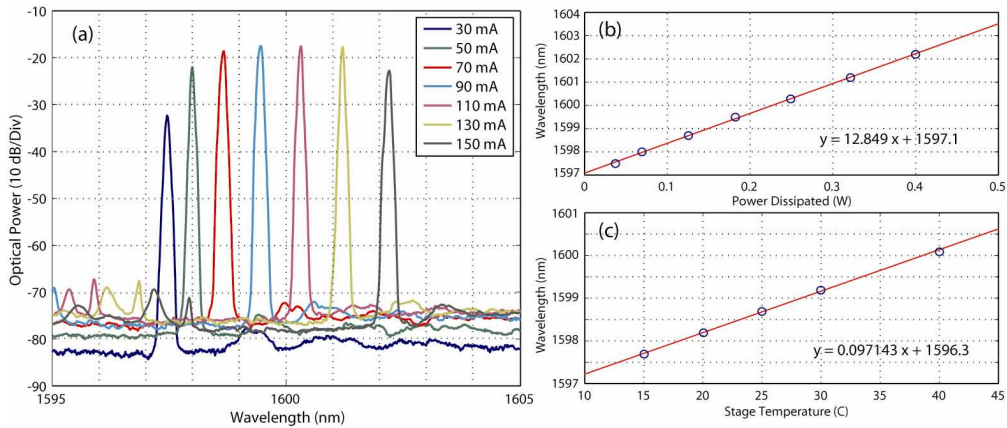


Fig. 6. (a) continuous wave lasing spectrum for various current levels. (b) Continuous wave lasing wavelength versus electrical dissipated power. (c) Pulsed lasing wavelength versus stage temperature.

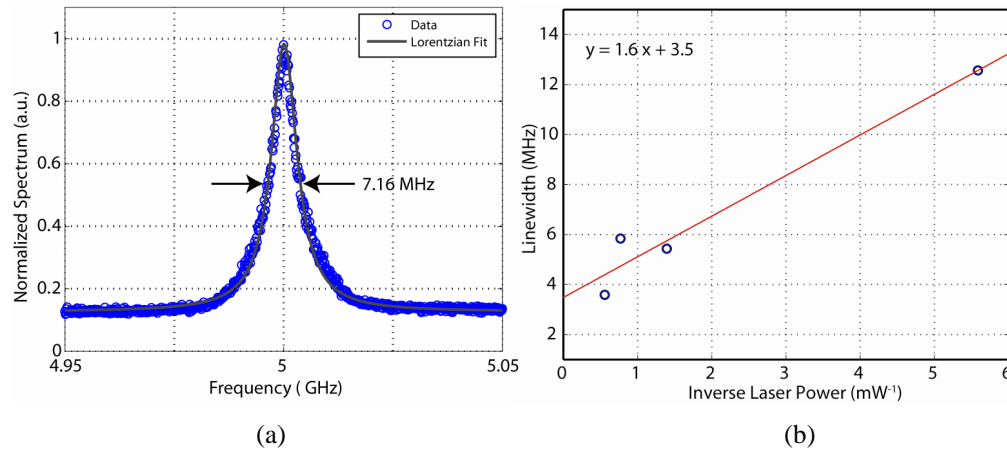


Fig. 7. (a) Delayed-self heterodyned line width trace at 1.8 mW laser output power. (b) The laser line width versus the inverse laser output power.

The laser line width is measured by using the delayed-self heterodyne method [11]. The laser light is collected into a lensed fiber and amplified with an L-band amplifier. The ASE from the L-Band amplifier is filtered out with a 5 nm wide tunable band pass filter. The light is then modulated with a lithium niobate modulator at 5 GHz to generate Lorentzian sidebands 5 GHz away from the laser signal. The signal is placed through a fiber interferometer with a 3.5 microsecond delay and then collected into a photodetector in HP lightwave analyzer. The down converted, line shape is measured at 5 GHz on the spectrum analyzer with a 50 KHz resolution bandwidth. Figure 7(a) shows minimum measured line width at 1.8 mW laser output power with a down converted Lorentzian line width of 7.16 MHz corresponding to a 3.6 MHz linewidth, a typical value for commercial DFB lasers. The line width versus inverse output power is shown in Fig. 7(b) with increased powers leading to narrower line widths.

4. Conclusion

We have demonstrated a single wavelength electrically pumped distributed feedback silicon evanescent laser operating at 1600 nm. The laser threshold is 25 mA, and has a maximum laser output of 5.4 mW at 10 °C with a maximum lasing temperature of 50 °C. The 50 dB of side mode suppression and 3.6 MHz line width, are comparable to commercial III-V DFB

lasers, and can be used in conjunction with high speed silicon modulators and low loss multiplexors to create wavelength division multiplexed transmitters on silicon.

Acknowledgments

The authors would like to thank D. Blumenthal, L. Coldren, M. Paniccia, H. Park, A. Ramaswamy, L. Johansson, R. Jones, M. Paniccia, J. Shah, and W. Chang for insightful discussions and B. Kim, and H.-W. Chen for help with device fabrication. This work was supported by a grant from Intel Corp. and from DARPA/MTO DODN program and ARL under award number W911NF-05-1-0175 and W911NF-04-9-0001.